

## Achievement of a High Fusion Triple Product and Steady State Sustainment in High $\beta_p$ ELMy H-mode Discharges in JT-60U

A. Isayama<sup>1)</sup>, Y. Kamada<sup>1)</sup>, N. Hayashi<sup>1)</sup>, T. Suzuki<sup>1)</sup>, T. Oikawa<sup>1)</sup>, T. Fujita<sup>1)</sup>, T. Fukuda<sup>1)</sup>, S. Ide<sup>1)</sup>, H. Takenaga<sup>1)</sup>, K. Ushigusa<sup>1)</sup>, T. Ozeki<sup>1)</sup>, Y. Ikeda<sup>1)</sup>, N. Umeda<sup>1)</sup>, H. Yamada<sup>2)</sup>, M. Isobe<sup>2)</sup>, Y. Narushima<sup>2)</sup>, K. Ikeda<sup>2)</sup>, S. Sakakibara<sup>2)</sup>, K. Yamazaki<sup>2)</sup>, K. Nagasaki<sup>3)</sup> and the JT-60 Team<sup>1)</sup>

1) Japan Atomic Energy Research Institute, Naka, Ibaraki 311-0193, Japan

2) National Institute for Fusion Science, Toki, Gifu 509-5292, Japan

3) Institute of Advanced Energy, Kyoto University, Gokasho, Uji, Kyoto 611-0011, Japan

e-mail contact of main author: isayama@naka.jaeri.go.jp

**Abstract.** This paper reports results on the progress in steady-state high- $\beta_p$  ELMy H-mode discharges in JT-60U. A fusion triple product  $n_D(0)\tau_E T_i(0)$  of  $3.1 \times 10^{20} \text{ m}^{-3} \cdot \text{s} \cdot \text{keV}$  under full non-inductive current drive has been achieved at  $I_p=1.8 \text{ MA}$ , which renews the record value of the fusion triple product under full non-inductive current drive by 50%. A high-beta plasma with  $\beta_N \sim 2.7$  has been sustained for 7.4 s ( $\sim 60\tau_E$ ), where the duration is determined only by the facility limit such as the capability of the poloidal field coils and the upper limit of the injection duration of neutral beams. Destabilization of neoclassical tearing modes (NTMs) has been avoided with good reproducibility by tailoring the current and pressure profiles. On the other hand, the real-time NTM stabilization system has been developed, where the detection of the center of magnetic island and the optimization of injection angle of electron cyclotron (EC) wave are done in real-time. By the application of this system, a 3/2 NTM has been completely stabilized in high beta region ( $\beta_p \sim 1.2$ ,  $\beta_N \sim 1.5$ ), and beta value and confinement enhancement factor have been improved by the stabilization.

### 1. Introduction

High  $\beta_p$  ELMy H-mode plasma is characterized by the weak positive shear with central safety factor above unity, which is compatible with the plasma in the standard operational scenario of the international thermonuclear experimental reactor (ITER). We have optimized the discharge scenario pursuing the steady-state plasmas with high-beta, high-confinement and high non-inductively driven current fraction [1-6]. Since the last IAEA conference, significant improvements have been made in facility: (a) increase in the capacity of poloidal field coils by 20%, (b) increase in beam energy  $E_{NNB}$  and injection power  $P_{NNB}$  of the negative-ion-based neutral beam (NNB) injection system [7], (c) increase in the number of gyrotrons (4 units in total) and generation power ( $\sim 1 \text{ MW/unit}$ ) in the electron cyclotron (EC) wave injection system [8] and (d) routine operation of the pellet injection system. From the operational point of view, one of the key issues for obtaining the high performance plasmas is to suppress neoclassical tearing modes (NTMs). We have adopted two approaches for the NTM suppression: (a) avoidance of destabilization through profile optimization and (b) stabilization by electron cyclotron current drive (ECCD) / electron cyclotron heating (ECH). For the NTM stabilization, real-time NTM stabilization system has been developed, which incorporates with the real-time equilibrium reconstruction.

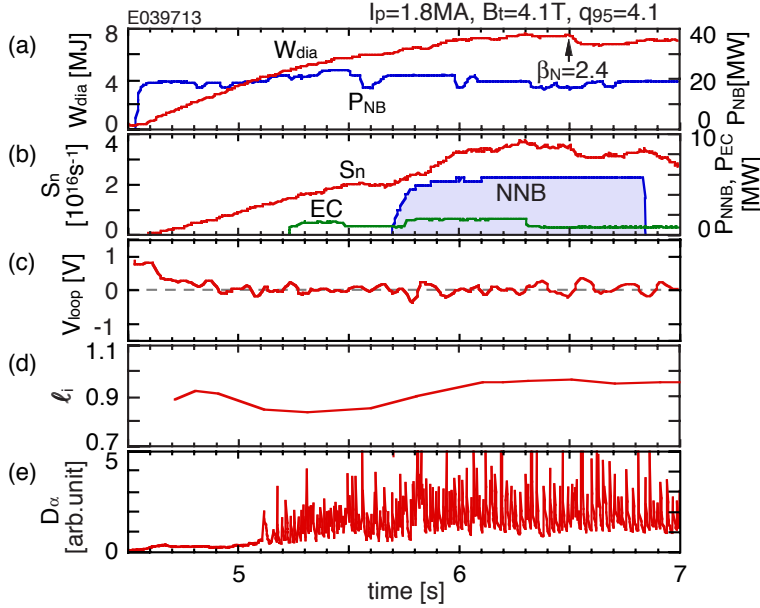


FIG. 1. Typical waveforms of a high  $\beta_p$  ELMy H-mode discharge: (a) stored energy and injection power of PNBs, (b) neutron emission rate, injection power of EC and NNB, (c) loop voltage, (d) internal inductance evaluated with MSE diagnostics, (e) intensity of  $D_\alpha$  line.

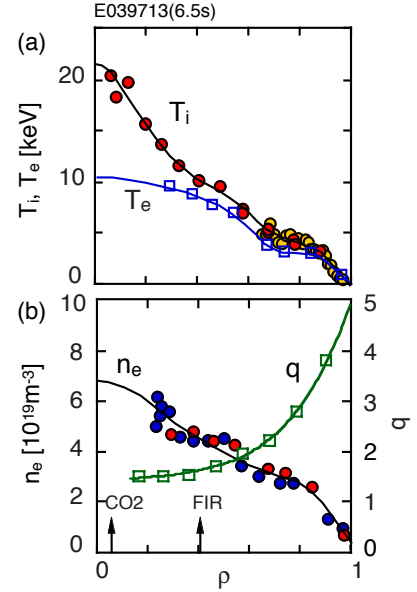


FIG. 2. Profiles at 6.5s in E39713: (a) ion and electron temperatures, (b) electron density and safety factor.

## 2. High Fusion Triple Product under Full Non-inductive Current Drive

We have performed the optimization of high  $\beta_p$  ELMy H-mode discharges, in which important issues are (a) simultaneous achievement of high-beta and high-confinement with high fraction of non-inductively driven current and (b) steady-state sustainment of the high performance plasma [1-6].

Typical waveforms of a high  $\beta_p$  ELMy H-mode discharge are shown in Fig. 1, where plasma parameters are as follows: plasma current  $I_p=1.8$  MA, toroidal field  $B_t=4.1$  T, major radius  $R=3.23$  m, minor radius  $a=0.78$  m, safety factor at the 95% flux surface  $q_{95}=4.1$  and triangularity at the separatrix  $\delta_x=0.34$ . In this discharge, NNB with  $E_{\text{NNB}}=402$  keV and  $P_{\text{NNB}}=5.7$  MW was injected from 5.7 s. At  $t=6.5$  s, a high-performance plasma with the following parameters was obtained: stored energy  $W_{\text{dia}}=7.5$  MJ, H-factor  $H_{89\text{PL}}=2.5$ , HH-factor  $\text{HH}_{y2}=1.2$ , poloidal beta  $\beta_p=1.7$ , normalized beta  $\beta_N=2.4$ , fusion triple product  $n_D(0)\tau_E T_i(0)=3.1 \times 10^{20} \text{ m}^{-3} \cdot \text{s} \cdot \text{keV}$  (Here,  $n_D(0)$ ,  $\tau_E$ ,  $T_i(0)$  are the central deuterium density, energy confinement time, the central ion temperature, respectively.) and equivalent fusion gain  $Q_{\text{DT}^{\text{eq}}}=0.185$ . Figures 1(c) and (d) suggest that plasma current is fully non-inductively driven. Note that in evaluating the internal inductance  $l_i$ , plasma equilibria were reconstructed by using the motional Stark effect (MSE) diagnostic. Profiles of ion temperature  $T_i$ , electron temperature  $T_e$ , electron density  $n_e$  and safety factor  $q$  at 6.5 s are shown in Fig. 2. Ion temperature was measured with charge exchange recombination spectroscopy, and electron temperature was measured with Thomson scattering. In evaluating the electron density, far-infrared interferometer with tangency radius of  $\rho \sim 0.4$ , tangential  $\text{CO}_2$  laser interferometer and Thomson scattering are used. The central safety factor  $q_0$  is kept above unity throughout the NB phase to avoid sawtooth oscillations.

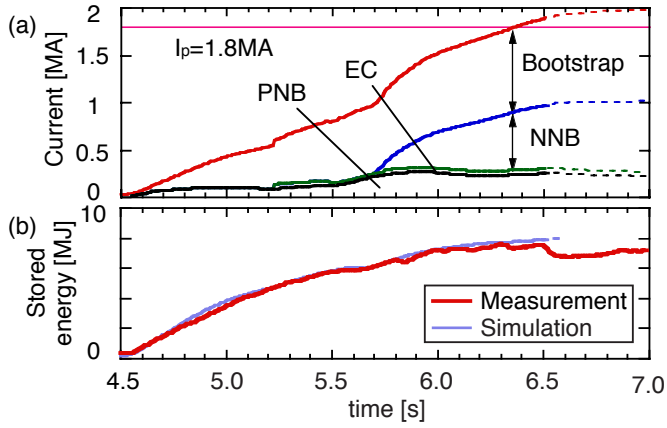


FIG. 3. (a) Time evolution of driven current in E39713 simulated with the TOPICS code, (b) Comparison of stored energy between measurement and simulation.

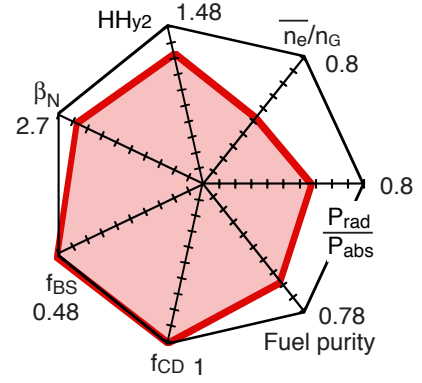


FIG. 4. Septangular plot of E39713 data. Values in this figure correspond to those in the steady-state weak positive shear scenario in ITER.

In order to validate the full non-inductive current drive, time evolution of the bootstrap current, beam-driven current was simulated using the time-dependent transport code TOPICS. The EC-driven current was evaluated using the Fokker-Planck code combined with the ray-tracing code. As shown in Fig. 3(a), plasma current is fully maintained by the non-inductively driven current. The result of simulation is validated by comparing the stored energy in experiment with simulation: as shown in Fig. 3(b), both agree well each other until the appearance of a mini-collapse at  $t=6.5$  s. Slowing-down of the NNB fast ions was also simulated with the Orbit Following Monte-Carlo (OFMC) code, which indicates that about 95% of energy and parallel momentum are transferred to the plasma in 0.8 s after the injection, suggesting that the plasma is nearly in steady state at  $t=6.5$  s. Fractions of the NB-driven current ( $f_{NB}$ ) and bootstrap current ( $f_{BS}$ ) are nearly equal, which is similar to the situation in the steady-state operation in ITER.

In order to visualize the integrated plasma performance, we have used the septangular plot (Fig. 4), which contains (a) normalized beta, (b) HH-factor, (c) line average electron density  $\bar{n}_e$  normalized by the Greenwald density  $n_G$ , (d) ratio of radiation power  $P_{rad}$  to absorption power  $P_{abs}$ , (e) fuel purity defined as the ratio of the number of deuterons to that of electrons, (f) fraction of bootstrap current, and (g) fraction of non-inductively driven

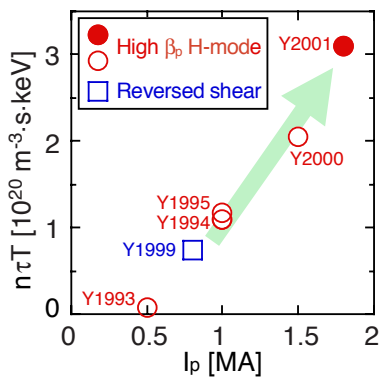


FIG. 5. Progress in fusion triple products under full non-inductive current drive.

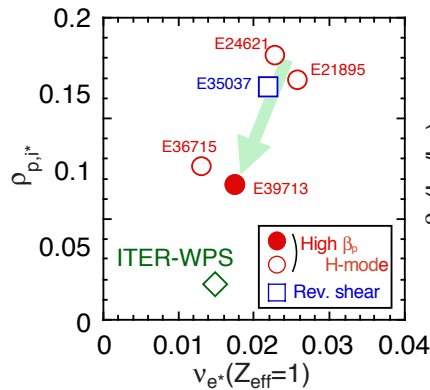


FIG. 6. Operational region plotted on  $\rho_{p,i^*} - v_{e^*}$  space.

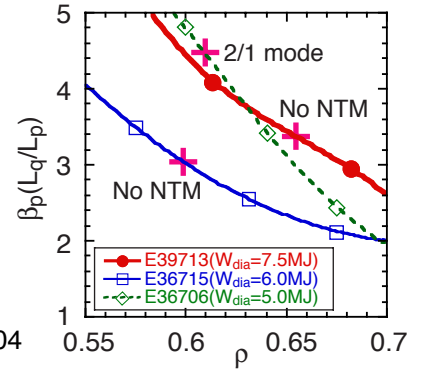


FIG. 7. Profiles of  $\beta_p(L_q/L_p)$  near the  $q=2$  surface. '+' symbol denotes the location of the  $q=2$  surface.

current fCD. In this plot, each value is normalized by that at ITER [9]. In E39713,  $\bar{n}_e/n_G=0.42$ ,  $P_{\text{rad}}/P_{\text{abs}}=0.54$ , fuel purity=0.6,  $f_{\text{CD}}=1$  and  $f_{\text{BS}}=0.49$ . The values of  $f_{\text{CD}}$  and  $f_{\text{BS}}$  meet the requirement at ITER, and  $\beta_N$  and  $\text{HH}_{\text{y2}}$  are close to the requirement ( $\geq 80\%$ ). Longer pulse duration with high density and high radiation fraction is a remaining issue.

Progress of  $n\tau T$  under full non-inductive current drive in high  $\beta_p$  H-mode and reversed shear discharges in JT-60U is shown in Fig. 5. The fusion triple product obtained in E39713 exceeds the previous record ( $2.0 \times 10^{20} \text{ m}^{-3} \cdot \text{s} \cdot \text{keV}$  under full non-inductive current drive) by as much as 50%. In figure 6, ion poloidal Larmor radius  $\rho_{p,i^*}$  is plotted against electron collisionality  $\nu_{e^*}$ . In evaluating  $\rho_{p,i^*}$  and  $\nu_{e^*}$ , we used volume average  $n_e$ , density weighted volume average  $T_i$  and  $T_e$ , poloidal field at the edge,  $q=2$ , effective ion charge  $Z_{\text{eff}}=1$ , inverse aspect ratio  $\varepsilon=0.5a/R$ . In E39713,  $\nu_{e^*}=0.017$  and  $\rho_{p,i^*}=0.067$ , and the values of  $\nu_{e^*}/\nu_{e^*}^{\text{ITER}}$  and  $\rho_{p,i^*}/\rho_{p,i^*}^{\text{ITER}}$  are 1.2 and 3.8, respectively ( $\nu_{e^*}^{\text{ITER}}$  and  $\rho_{p,i^*}^{\text{ITER}}$  are  $\nu_{e^*}$  and  $\rho_{p,i^*}$  at ITER, respectively). Accordingly, it indicates that the above result was obtained near the operational region of ITER.

In this series of discharges, NTMs with  $m/n=3/2$  and  $2/1$ , which appear even at  $q_0>1$ , limit the sustainment of high beta values. Here,  $m$  and  $n$  are poloidal and toroidal mode numbers, respectively. Destabilization of NTMs is avoided by optimizing the current and pressure profiles with good reproducibility so that steep pressure gradient is not located at the mode rational surfaces. As shown in Fig. 2, the  $q=1.5$  surface is located near the center of the plasma where the pressure gradient is small, which is effective in avoiding the  $3/2$  mode. As for the  $2/1$  mode, we have attempted to decrease the value of  $\beta_p(L_q/L_p)$ , which is one of the measures for the onset of neoclassical tearing modes ( $L_q=q/(dq/dr)$ ,  $L_p=p/(dp/dr)$ ;  $\beta_p$  is evaluated using local parameters). In Fig. 7, profiles of  $\beta_p(L_q/L_p)$  in several discharges are displayed ( $q_{95}=4.1-4.75$ ). Note that high  $\beta_N$  ( $\sim 2.5$ ) and high  $n\tau T$  were sustained without NTM in shot E36715, and that the  $2/1$  mode was destabilized in shot E36706. In shot E39713, the value of  $\beta_p(L_q/L_p)$  at the  $q=2$  surface ('+' symbol in Fig. 7) is kept as low as that in E36715 even at higher stored energy by making the  $q$ -profile broader. Accordingly, the profile optimization is thought to be effective in avoiding the destabilization of NTMs.

### 3. Steady-state Sustainment of High-beta Plasmas

Demonstration of the steady-state sustainment of high-beta plasmas is important to investigate the phenomena which might manifest corresponding to the time scale of current diffusion. The current diffusion time in a high  $\beta_p$  H-mode discharge is an order of 10 s in JT-60U due to its large size and high temperature. Such a long-pulse and high- $\beta$  discharge has been realized by the improvement in the poloidal coil power supply: a high triangularity plasma with  $\delta_x \sim 0.45$  can be sustained for 10 s, which duration also corresponds to the maximum pulse width of the neutral beams in JT-60U.

Typical waveforms of a long-pulse high- $\beta_p$  ELMy H-mode discharge are shown in Fig. 8. Plasma parameters are as follows:  $I_p=1.0$  MA,  $B_t=1.8$  T,  $q_{95}=3.3$ ,  $\delta_x \sim 0.45$ . NB power was gradually increased by the stored energy feedback in order to avoid the  $2/1$  mode and large-amplitude  $3/2$  mode, which cause serious confinement degradation. Deuterium pellets

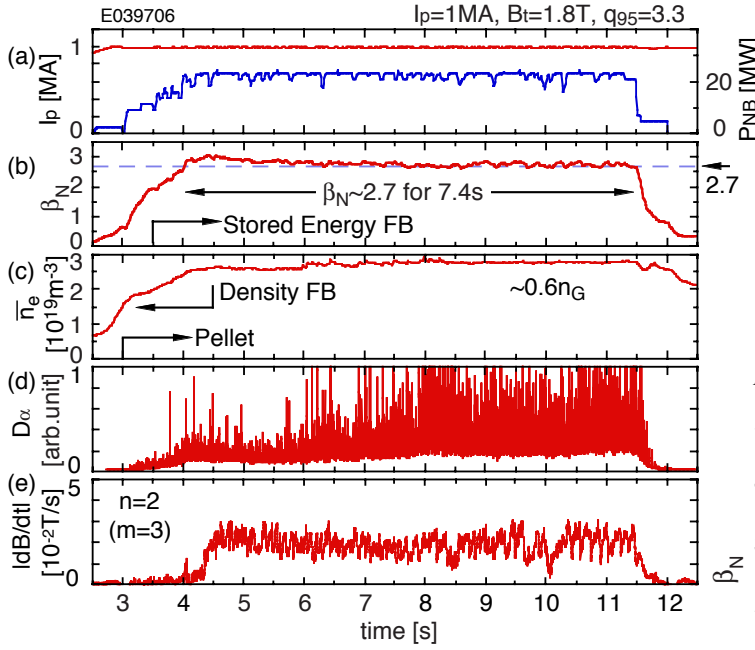


FIG. 8. Typical waveforms of a long-pulse high  $\beta_p$  ELMy H-mode discharge: (a) plasma current and NB injection power, (b) normalized beta, (c) line average electron density, (d) intensity of  $D_\alpha$  line, (e) amplitude of magnetic perturbations with  $n=2$ .

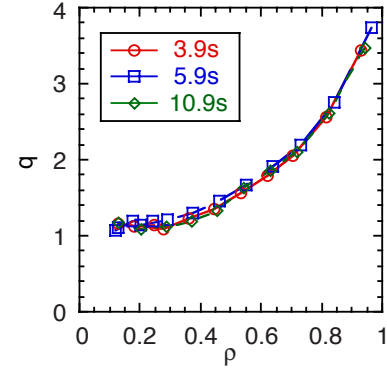


FIG. 9. Safety factor profiles in E39706.

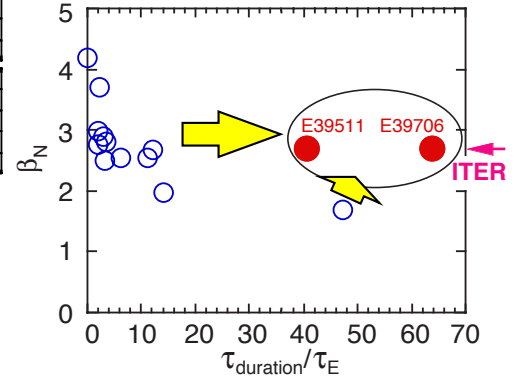


FIG. 10. Progress in long-pulse discharge:  $\beta_N$  versus  $\tau_{\text{duration}}/\tau_E$ .

were injected from the high-field side at 120 m/s, 10 Hz from  $t=3$  s, which contribute to obtaining a high density plasma without significant confinement degradation. The pellet injection also contributes to keeping core density for reducing the shine-through loss power, which is small ( $\lesssim 10\%$ ) but becomes important in the long-pulse operation. Although a  $3/2$  mode started to grow at  $t=4.3$  s ( $\beta_N \sim 2.9$ ), normalized beta was kept almost stationary and no continuous degradation was observed, and an ELMy H-mode plasma with  $\beta_N \sim 2.7$  and  $\beta_p \sim 1.5$  was sustained for 7.4 s, which corresponds to  $\sim 60\tau_E$ . Here, the duration is determined by the facility constraint. In E39706, total NB injection power reaches 180 MJ, but no significant increase in the  $D_\alpha$  signal and the impurity content was observed. As shown in Fig. 9, safety factor profile is almost identical, and the central safety factor is kept above unity during the NB phase. This fact was also confirmed by electron temperature perturbations measured with electron cyclotron emission (ECE) diagnostics: no sawtooth is observed, and the location of the magnetic island corresponding to the  $3/2$  mode is almost unchanged.

Figure 10 shows the value of  $\beta_N$  against duration  $\tau_{\text{duration}}$  normalized by  $\tau_E$  in typical high  $\beta_p$  ELMy H-mode discharges in JT-60U. In shot E39511 ( $I_p=1$  MA,  $B_t=2$  T,  $q_{95}=3.6$ ), a high-performance plasma with  $\beta_N=2.7$ ,  $\beta_p=1.6$ ,  $H_{89PL}=1.8$ ,  $HH_{y2}=0.89$ ,  $\bar{n}_e/n_G=0.67$  was sustained for 6.5 s. It is obvious that the operational region has been significantly extended by these discharges: High value of  $\beta_N$ , which is comparable to that in ITER, was obtained in larger  $\tau_{\text{duration}}/\tau_E$  region.

#### 4. Real-time NTM Stabilization

Stabilization of NTMs by EC is important to sustain high beta plasmas. In JT-60U, it was demonstrated that the 3/2 NTM can be completely stabilized by injecting the fundamental O-mode EC wave to the center of the magnetic island [10]. At the same time, it has been found that the precise adjustment of EC injection angle is indispensable in order to achieve the complete stabilization. In case the deposition location is misaligned by only about half of the island width ( $\sim$ several centimeters), the stabilization effect by EC was significantly decreased.

When EC is used as a tool for the NTM stabilization in a future device such as ITER, NTMs are needed to be detected and stabilized in real-time, since the optimum injection angle changes in time. In JT-60U, we developed a real-time NTM stabilization system and demonstrated that the center of the magnetic island can be detected from the electron temperature perturbation profile. In 2002, extensive development has been made in the real-time control system, where the plasma shape is first reconstructed in real-time (every 10 ms) with the Cauchy condition surface (CCS) method [11], and the mode location is coarsely estimated. Subsequently, fine tuning is performed by evaluating the electron temperature perturbation profile, utilizing the fact that an M-shaped perturbation profile shown in Fig. 13 is obtained at the magnetic island and that the center of the island corresponds to the local minimum point of the profile. In obtaining the perturbation profile, standard deviation of the ECE heterodyne radiometer signal is evaluated. This evaluation method has the advantage that the mode amplitude can be obtained without evaluating the mode frequency.

Typical waveforms of the NTM stabilization experiment are shown in Fig. 11. Plasma parameters of this discharge are as follows:  $I_p=1.5$  MA,  $B_t=3.7$  T,  $R=3.3$  m,  $a=0.78$  m,  $q_{95}=3.8$ . A 3/2 NTM was destabilized at  $\beta_N \sim 1.5$  by the NB injection power of  $\sim 20$  MW. The mode amplitude gradually decreased after 3 MW EC injection at  $t=7.56$  s ( $H_{89PL}=1.8$ ,  $HH_{y2}=1.0$ ), and the 3/2 mode was completely stabilized at 8.8 s. Even after the turn-off of the EC injection at 9.5 s, the 3/2 mode did not appear and  $\beta_N$  continued to increase to 1.67. Since NB injection power was fixed, this shows confinement improvement. In fact,  $H_{89PL}$  and  $HH_{y2}$  increase to 1.9 and 1.1, respectively. At  $t=10.8$  s, the 3/2 mode reappeared, and  $\beta_N$  and  $\bar{n}_e$  decreased. Profiles of electron temperature at  $t=7.5$  s (just before EC), 9.4 s (after the stabilization), 10.7 s (just before the mode reappearance) and 11.5 s are shown in Fig. 12. It is shown that a flat region is formed at  $R=3.65-3.7$  m suggesting the formation of magnetic island, and  $T_e$  inside the mode rational surface is affected by the NTM. An increase of  $\beta_N$  by the stabilization is 11% and degradation due to the NTM reappearance is 13%. These values are comparable to the prediction of the island model ( $\sim 13\%$ ) by Chang et al.[12].

Figure 11(e) shows time traces of channel number of the heterodyne radiometer. The value for  $X_{CCS}$  corresponds to the channel number at the mode rational surface evaluated with the CCS method, and  $X_{min}$  corresponds to the location at which the perturbation level reaches the local minimum. The value of  $X_{CCS}$  stays at channel 8 since the plasma position is fixed. The real-time system functions in a way that EC angle is changed and EC is injected at

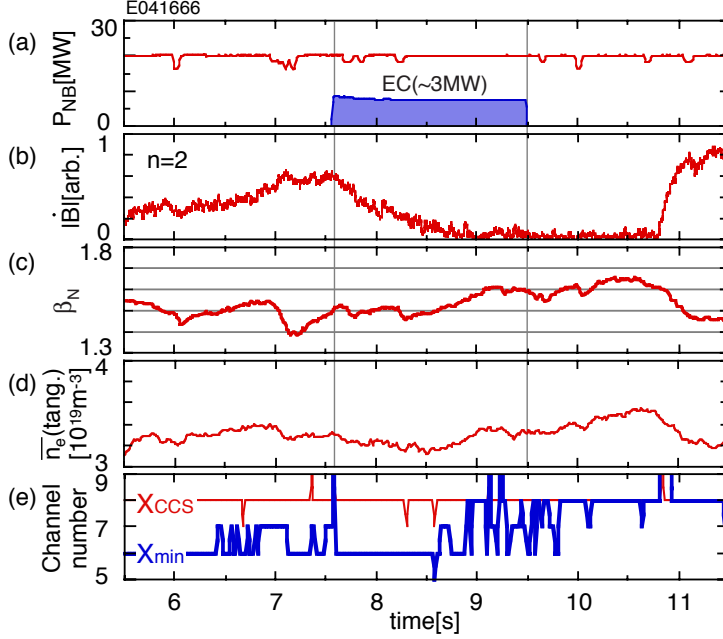


FIG. 11. Typical waveforms of a real-time NTM stabilization experiment: (a) injection power of NBs and EC, (b) amplitude of magnetic perturbations with  $n=2$ , (c) normalized beta, (d) line average electron density, (e) channel number of the heterodyne radiometer.

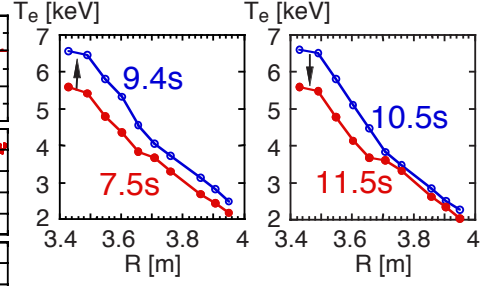


FIG. 12. Profiles of electron temperature at 7.5s, 9.4s, 10.5s and 11.5s in E41666.

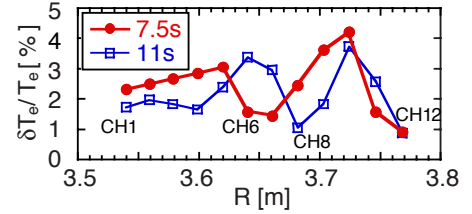


FIG. 13. Amplitude profiles of electron temperature perturbations at 7.5s and 11s.

the flux surface corresponding to  $X_{\min}$ . The validity of this function is confirmed by the amplitude profile depicted in Fig. 13: the local minimum is actually located at channel 6 or 7 at  $t=7.5$  s. The island center is located at  $R=3.68$  m at  $t=11$ s, which indicates that the mode rational surface has changed its location. The real-time system recognizes the change and indicates that the island center is located at channel 8.

The ratio of the EC-driven current to the bootstrap current at the mode rational surface is an important parameter as a measure of the efficiency of the stabilization. According to the Fokker-Planck code and the ACCOME code, the maximum EC-driven current density at the mode rational surface is comparable to the bootstrap current density ( $\sim 0.25$  MA/m<sup>2</sup>), which shows that the stabilization was effectively accomplished.

Time evolution of the amplitude of electron temperature perturbations  $\tilde{T}_e$  is shown in Fig. 14, where  $\tilde{T}_e$  is measured at 2 cm intervals. The brighter region corresponds to the region with large mode amplitude. The 'valley' of the contour plot corresponds to the center of the island. One can see that the center of the island is slightly meandering in time. After the EC injection, the mode amplitude at the high field side rapidly decreases, while it is not the case at the low field side. This shows asymmetry in the perturbation profile. It is also noteworthy that the amplitude at the low field side increases after the EC injection for  $\sim 100$  ms. As time goes on, the mode amplitude at the low-field side decreases and at the same time island width ( $\sim$ distance between the two peaks) also decreases. At  $t=8.4$ s, the island width rapidly decreases. This behavior is consistent with the description of the modified Rutherford equation, as shown in Fig. 15:  $dw/dt \ll 0$  for  $w \leq 0.05$  ( $w$  is island width.). It should be also noted that the increase in beta and density starts at 8.3–8.5 s (Fig. 12), which is close to the time of the quick shrink.

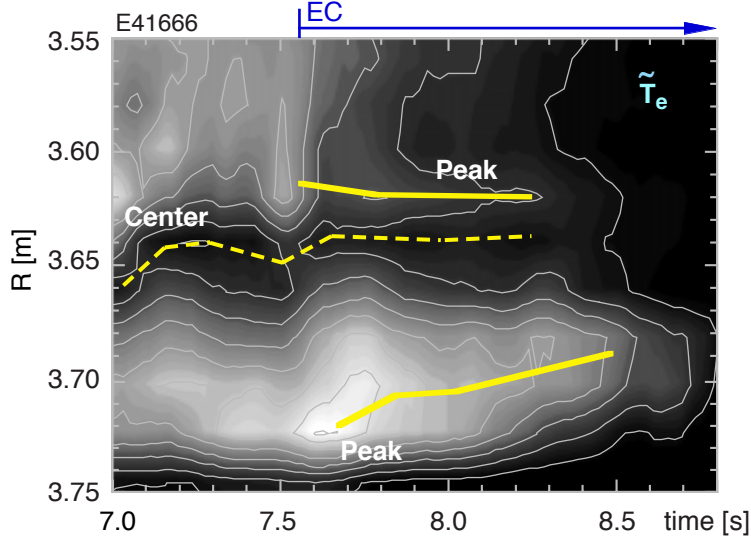


FIG. 14. Contour plot of electron temperature perturbation near the magnetic island.

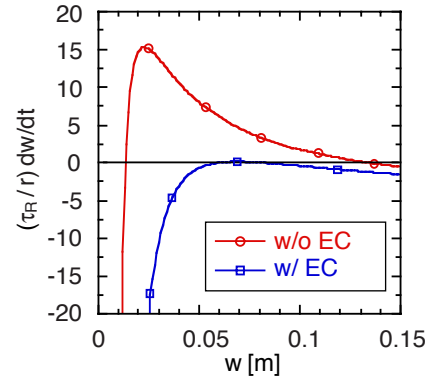


FIG. 15. Plot of  $(\tau_R/r) dw/dt$  against  $w$  based on the modified Rutherford equation.  $\tau_R$  is the resistive time scale.

## 5. Conclusions

In the high  $\beta_p$  ELMy H-mode discharges, we have obtained the following results:

- Highest fusion triple product of  $3.1 \times 10^{20} \text{ m}^{-3} \cdot \text{s} \cdot \text{keV}$  under full non-inductive current drive has been obtained at  $I_p=1.8 \text{ MA}$ ,  $B_t=4.1 \text{ T}$ ,  $q_{95}=4.1$ . Values of collisionality and poloidal Larmor radius are close to those at ITER ( $v_{e*}/v_{e*}^{\text{ITER}} \sim 1$ ,  $\rho_{p,i*}/\rho_{p,i*}^{\text{ITER}} \sim 4$ ). In the same series of discharges, destabilization of NTMs has been avoided with good reproducibility through the optimization of current and pressure profiles.
- A high beta plasma with  $\beta_N=2.7$ ,  $\beta_p=1.5$  has been sustained for 7.4 s at  $q_{95}=3.3$ . The duration time of high beta extends to  $\sim 60\tau_E$ , which is limited by the facility capability.
- Real-time NTM stabilization system, where the identification of the mode location and the feedback control of EC injection angle are performed in real-time, has been developed. By using this system, a 3/2 NTM in high beta region ( $\beta_N=1.5$ ,  $\beta_p=1.1$ ;  $B_t=3.7 \text{ T}$ ) has been completely stabilized, and beta value and H-factor have increased spontaneously after the stabilization.

## References

- [1] KAMADA, Y., et al., Proc. 15th Int. Conf. Fusion Energy, Seville 1994 (IAEA, Vienna, 1995) vol 1, p 651.
- [2] KAMADA, Y., et al., Proc. 16th Int. Conf. Fusion Energy, Montreal 1996 (IAEA, Vienna, 1997) vol 1, p 247.
- [3] KAMADA, Y., et al., Nucl. Fusion **39** (1999) 1845.
- [4] ISAYAMA, A., et al., Nucl. Fusion **41** (2001) 761.
- [5] OIKAWA, T., et al., Nucl. Fusion **41** (2001) 1575.
- [6] KAMADA, Y., et al., Fusion Sci. Technol. **42** (2002) 185.
- [7] UMEDA, N., et al., this conference; IAEA-CN-94/CT-6Rd.
- [8] SUZUKI, T., et al., this conference; IAEA-CN-94/EX/W-2.
- [9] in 'Plant Design Specification and Plant Description Document' (G A0 FDR 1 00-11-16 W 0.1) Vol.1 Chap. 4.
- [10] ISAYAMA, A., et al., Plasma Phys. Control. Fusion **42** (2000) L37.
- [11] KURIHARA, K., et al., Fusion Eng. Design **51-52** (2000) 1049.
- [12] CHANG, Z., et al., Nucl. Fusion **34** (1994) 1309.